Journal of Biomolecular NMR, **11:** 451–456, 1998.
KLUWER/ESCOM

CO_H(N)CACB experiments for assigning backbone resonances in $^{13}C/^{15}N$-labeled proteins

Nathan Astrof[a], Clay Bracken[b], John Cavanagh[c] and Arthur G. Palmer III[b,*]
[a]*Department of Chemistry and* [b]*Department of Biochemistry and Molecular Biophysics, Columbia University, 630 West 168th Street, New York, NY 10032, U.S.A.* [c]*NMR Structural Biology Facility, Wadsworth Center, New York State Department of Health, Albany, NY 12201, U.S.A.*

Received 3 December 1997; Accepted 26 January 1998

Key words: constant time evolution, heteronuclear NMR, proteins, sequential assignments, triple resonance

Abstract

A triple resonance NMR experiment, denoted CO_H(N)CACB, correlates $^{1}H^{N}$ and ^{13}CO spins with the $^{13}C^{\alpha}$ and $^{13}C^{\beta}$ spins of adjacent amino acids. The pulse sequence is an 'out-and-back' design that starts with $^{1}H^{N}$ magnetization and transfers coherence via the ^{15}N spin simultaneously to the ^{13}CO and $^{13}C^{\alpha}$ spins, followed by transfer to the $^{13}C^{\beta}$ spin. Two versions of the sequence are presented: one in which the ^{13}CO spins are frequency labeled during an incremented t_1 evolution period prior to transfer of magnetization from the $^{13}C^{\alpha}$ to the $^{13}C^{\beta}$ resonances, and one in which the ^{13}CO spins are frequency labeled in a constant-time manner during the coherence transfer to and from the $^{13}C^{\beta}$ resonances. Because ^{13}CO and ^{15}N chemical shifts are largely uncorrelated, the technique will be especially useful when degeneracy in the $^{1}H^{N}$-^{15}N chemical shifts hinders resonance assignment. The CO_H(N)CACB experiment is demonstrated using uniformly $^{13}C/^{15}N$-labeled ubiquitin.

Heteronuclear triple resonance experiments have significantly expanded the scope and utility of NMR for the structural and dynamic characterization of proteins, nucleic acids, and their respective complexes. For many proteins of molecular weight <15 kDa, a single pair of experiments, the HNCACB (Wittekind and Mueller, 1993) and CBCA(CO)NH (Grzesiek and Bax, 1993b), are sufficient to establish the majority of the protein backbone resonance assignments. The sequence-specific assignment of a series of correlated residues is facilitated because the chemical shifts of the $^{13}C^{\alpha}$ and $^{13}C^{\beta}$ resonances are sensitive to amino acid type (Grzesiek and Bax, 1993b). Although these experiments offer good resolution, resonance overlap due to chemical shift degeneracy may still occur and impede resonance assignments.

In this communication, we present a method to establish sequential protein resonance assignments by correlation of the intraresidue (i) and interresidue (i − 1) $^{13}C^{\alpha}$ and $^{13}C^{\beta}$ chemical shifts with the $^{13}CO_{(i-1)}$ and $^{1}H^{N}_{(i)}$ chemical shifts. The CO_H(N)CACB experiment is derived from the HNCACB (Wittekind and Mueller, 1993) and COHNNCA (Szyperski et al., 1995) experiments. The process of establishing resonance assignments using the CO_H(N)CACB and HNCACB techniques is similar. However, backbone ^{13}CO and ^{15}N chemical shifts are essentially uncorrelated; thus, assignments for residues with overlapping $^{1}HN_{(i)}$, $^{15}N_{(i)}$ chemical shifts may be obtained using the new technique. Detection of the $^{1}H^{N}$ signal in both the HNCACB and CO_H(N)CACB experiments facilitates comparisons between the two spectra. Furthermore, ^{13}CO chemical shifts (Wishart et al., 1991) and coupling constants (Löhr et al., 1997) can be useful for establishing protein secondary structure and the measurement of the ^{13}CO relaxation rates (Engelke and Rüterjans, 1997) can complement ^{15}N relaxation investigations of protein dynamics (Palmer, 1997).

The pulse sequence for the CO_H(N)CACB experiment is shown in Figure 1 and incorporates many features of previously published experiments that utilize the frequency labeling of the ^{13}CO spin by 'out-and-

* To whom correspondence should be addressed

DISK Gr.: 201022148, PIPS Nr. 162899 (jnmrkap:bio2fam) v.1.1
jnmr541.tex; 4/06/1998; 15:29; p.1

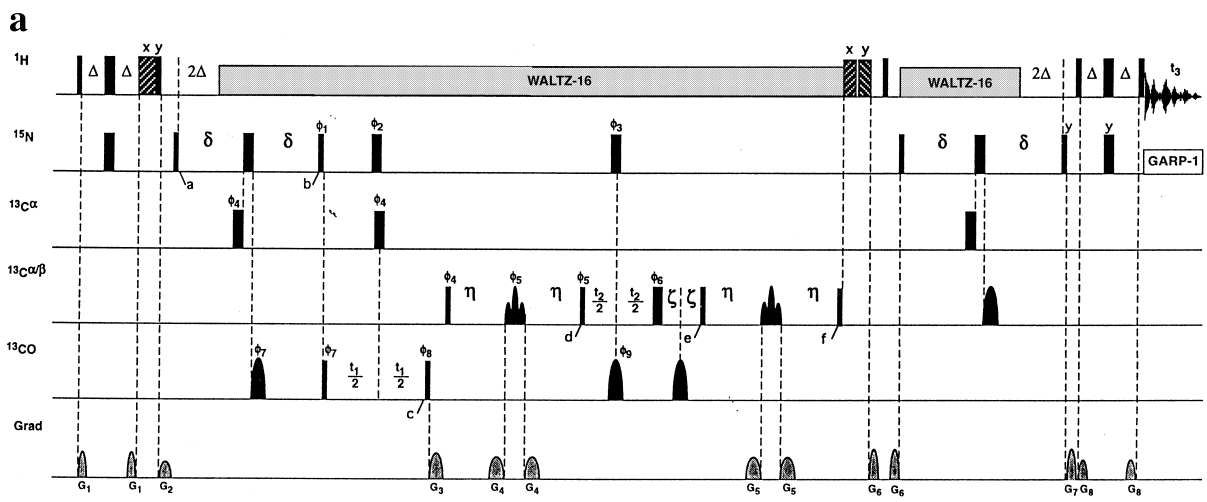

Figure 1. 3D CO_H(N)CACB pulse sequences using (a) an incremented t_1 evolution period and (b) a constant time t_1 evolution period. The fixed delays were set as follows (Wittekind and Mueller, 1993; Szyperski et al., 1995): $\Delta = 2.7$ ms, $\delta = 13.5$ ms, and $\eta = 4.0$ ms. In (a), the initial value of the incremented delay period t_2 was set equal to 2ζ. In (b), the initial value of the incremented delay period t_1 was set equal to ζ. The 90° and 180° pulses are represented by thin and thick bars, respectively; shaped 180° pulses are represented by solid half ovals; band selective pulses are drawn with three lobes; and radio frequency spin-locks are represented by striped bars. The magnetic field gradients are represented by shaded half ovals. Pulses applied at the $^{13}C^{\alpha}/^{13}C^{\alpha/\beta}$ and ^{13}CO resonance frequencies were adjusted to provide a null at the corresponding ^{13}CO or $^{13}C^{\alpha}/^{13}C^{\alpha/\beta}$ frequencies. The square ^{13}CO or $^{13}C^{\alpha/\beta}$ 90° and 180° pulses were set to 48.2 μs and 43 μs, respectively. The square $^{13}C^{\alpha}$ 180° pulses were set to 48.6 μs. The shaped 180° ^{13}CO pulses were applied with 4% truncated Gaussian profiles using a peak field strength of 5.8 kHz and a duration of 86 μs. In (a), a $^{13}C^{\alpha/\beta}$ band-selective 180° REBURP pulse (Geen and Freeman, 1991) was applied with a peak field strength of 15.7 kHz and a duration of 400 μs. In (b), a $^{13}C^{\alpha/\beta}$ band selective 180° rSNOB pulse was applied with a peak field strength of 15.7 kHz and a duration of 149 μs (Kupče et al., 1995). The shaped 180° ^{13}CO pulse used in the t_2 evolution period of (b) had a 4% truncated Gaussian amplitude profile with a peak field strength of 11.6 kHz and a duration of 86 μs. This pulse is modulated as $\exp[i(\omega_{C'} - \omega_{rf})t]\cos[(\omega_{C'} - \omega_{C^{\alpha/\beta}})t]$, in which $\omega_{C'}$ and $\omega_{C^{\alpha/\beta}}$ are the centers of the ^{13}CO and $^{13}C^{\alpha/\beta}$ spectral ranges, ω_{rf} is the frequency of the rf carrier used for the pulse, and t ranges from 0 to the length of the pulse. The value of ω_{rf} will depend on whether separate rf transmitters are used to generate ^{13}CO and $^{13}C^{\alpha/\beta}$ pulses. Proton hard pulses were applied with a 25 kHz field strength; WALTZ-16 decoupling (Shaka et al., 1983) of ^{1}H spins was achieved using a field strength of 3.6 kHz. GARP-1 decoupling (Shaka et al., 1985) of ^{15}N spins was achieved using a field strength of 1.25 kHz. Water suppression was obtained using spin-lock purge pulses (Messerle et al., 1989).The spin-lock pulses were applied at 25 kHz field strength for durations of 0.5 ms, 0.8 ms and 1.0 ms, listed in order of appearance in the pulse sequences. Unless indicated otherwise, pulses are applied with x phase. The phase cycling for sequence (a) was as follows: $\phi_1 = 2(x),2(-y)$; $\phi_2 = 4(x),4(-x)$; $\phi_3 = 8(x),8(-x)$; $\phi_4 = 4(x),4(-x)$; $\phi_5 = y$; $\phi_6 = 4(x),4(-x),4(y),4(-y)$; $\phi_7 = x,-x$; $\phi_8 = 52°$; $\phi_9 = 2(x),2(-x)$; and $\phi_{rec} = x,2(-x),x,2(-x,2(x),-x),x,2(-x),x$. Frequency discrimination in the $t_1(^{13}CO)$ and $t_2(^{13}C^{\alpha/\beta})$ dimensions was achieved using States-TPPI phase cycling (Marion et al., 1989b) of the pulse phases ϕ_7 for the $t_1(^{13}CO)$ indirect dimension and pulse phases ϕ_4 and ϕ_5 for the $t_2(^{13}C^{\alpha/\beta})$ indirect dimension. The gradients were applied as a sinusoidal function from 0 to π with the following durations and peak strengths: $G_1 = 1$ ms with $g_z = 7$ G/cm, $G_2 = 1.5$ ms with $g_x = 13.8$ G/cm, $G_3 = 1.5$ ms with $g_x = 13.8$ G/cm, $G_4 = 0.5$ ms with $g_z = 10.5$ G/cm, $G_5 = 2$ ms with $g_y = 10.2$ G/cm, $G_6 = 1.5$ ms with $g_x = 20.7$ G/cm, $g_z = 14$ G/cm, $G_7 = 2$ ms with $g_x = 7$ G/cm, $G_8 = 1$ ms with $G_x = 6.9$ G/cm, $G_y = 2.6$ G/cm. The phase cycling for sequence (a) was as follows: $\phi_1 = 2(x),2(-x)$; $\phi_2 = 4(x),4(-x)$; $\phi_3 = y$; $\phi_4 = 8(x),8(-x),8(y),8(-y)$; $\phi_5 = x,-x$; $\phi_6 = 2(x),2(-x)$; $\phi_7 = 4(x),4(-x),4(y),4(-y)$; $\phi_8 = 52°$; and $\phi_{rec} = x,2(-x),x,2(-x,2(x),-x),x,2(-x),x$. The receiver phase is inverted after 16 steps of the phase cycle. Frequency discrimination in the $t_1(^{13}CO)$ and $t_2(^{13}C^{\alpha/\beta})$ dimensions was achieved using States-TPPI phase cycling (Marion et al., 1989b) of the pulse phases ϕ_5 for the $t_1(^{13}CO)$ indirect dimension and pulse phases ϕ_2 and ϕ_3 for the $t_2(^{13}C^{\alpha/\beta})$ indirect dimension. The gradients were applied as a sinusoidal function from 0 to π with the following durations and peak strengths: $G_1 = 1$ ms with $g_z = 7$ G/cm, $G_2 = 1.5$ ms with $g_x = 13.8$ G/cm, $G_3 = 2$ ms with $g_x = 7$ G/cm, $G_4 = 1$ ms with $g_x = 6.9$ G/cm, $g_y = 2.6$ G/cm.

back' coherence transfer from the $^{1}H^{N}$ spin (Kay et al., 1990; Clubb et al., 1992; Wittekind and Mueller, 1993; Szyperski et al., 1995). The magnetization pathway is illustrated in Figure 2 and is described using the product operator formalism (Packer and Wright, 1983; Sørensen et al., 1983; van de Ven and Hilbers, 1983); only terms contributing to the desired signal are presented and the effects of relaxation are not considered. The symbols $H_{(i)\zeta}$, $N_{(i)\zeta}$, $C^{\alpha}_{(i)\zeta}$, $C^{\beta}_{(i)\zeta}$ and $C'_{(i)\zeta}$ (ζ =x, y, z) represent the Cartesian spin operators for the $^{1}H^{N}$, ^{15}N, $^{13}C^{\alpha}$, $^{13}C^{\beta}$ and ^{13}CO spins of the ith amino acid residue, respectively. The spin operators described in the text are those generated using pulse phases corresponding to the first step of the phase cycle, given in the caption to Figure 1. Pulses applied at the center of the $^{13}C^{\alpha}$ spectral window are designated

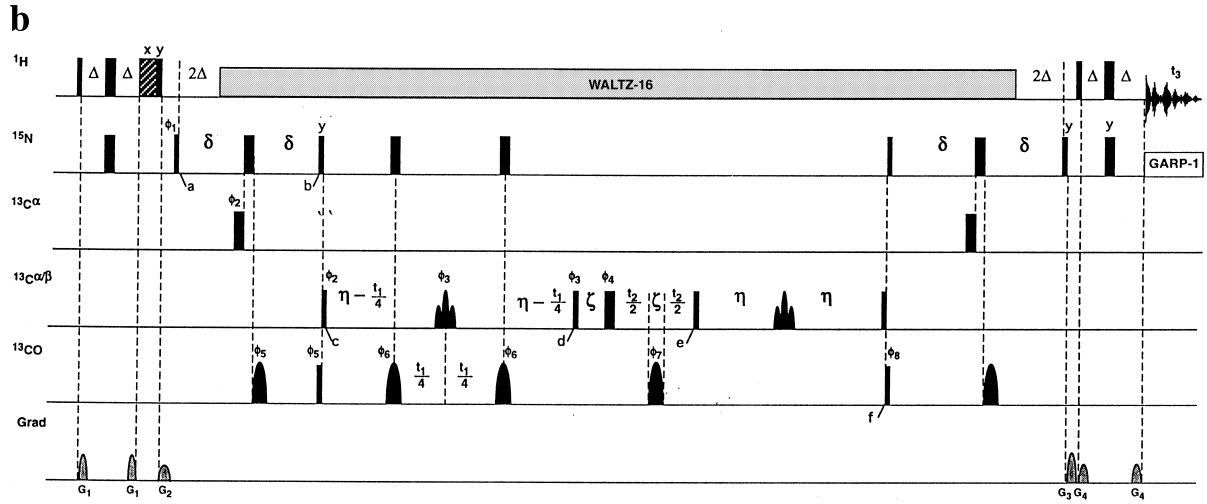

Figure 1. Continued.

$^{13}C^{\alpha}$ pulses and pulses applied between the $^{13}C^{\alpha}$ and the $^{13}C^{\beta}$ regions are designated $^{13}C^{\alpha/\beta}$ pulses.

Figure 1a illustrates a version of the experiment that employs a standard incremented t_1 period for ^{13}CO frequency labeling. Initially, longitudinal ^{1}H magnetization becomes anti-phase with respect to the attached ^{15}N by an INEPT (Morris and Freeman, 1979) sequence. At point a, the density operator is given by:

$$\sigma_a = -2H_{(i)z}N_{(i)y} \tag{1}$$

During the delay 2Δ, antiphase ^{15}N coherence becomes in-phase with respect to its directly attached proton; subsequent evolution due to the proton-heteronuclear scalar coupling is prevented by application of WALTZ-16 decoupling (Shaka et al., 1983). The ^{15}N magnetization evolves simultaneously under the $^{1}J_{NC'}$, $^{1}J_{NC^{\alpha}}$, and $^{2}J_{NC^{\alpha}}$ scalar couplings during a total duration 2δ. At point b, the density operator is given by:

$$\begin{aligned}\sigma_b = &-4N_{(i)x}C^{\alpha}_{(i)z}C'_{(i-1)z}\Gamma_{(i)}(\delta)\\ &-4N_{(i)x}C^{\alpha}_{(i-1)z}C'_{(i-1)z}\Gamma_{(i-1)}(\delta)\end{aligned} \tag{2}$$

in which

$$\begin{aligned}\Gamma_{(i)}(\delta) &= \sin(2\pi^{1}J_{NC'}\delta)\sin(2\pi^{1}J_{NC^{\alpha}}\delta)\\ &\quad\times\cos(2\pi^{2}J_{NC^{\alpha}}\delta)\\ \Gamma_{(i-1)}(\delta) &= \sin(2\pi^{1}J_{NC'}\delta)\cos(2\pi^{1}J_{NC^{\alpha}}\delta)\\ &\quad\times\sin(2\pi^{2}J_{NC^{\alpha}}\delta)\end{aligned} \tag{3}$$

Two-spin terms $2N_{(i)y}C'_{(i-1)z}$ and four-spin terms $8N_{(i)y}C^{\alpha}_{(i-1)z}C^{\alpha}_{(i)z}C'_{(i-1)z}$ that also develop are suppressed by the phase cycle ϕ_1.

The ^{15}N coherence that is antiphase with respect to the $^{13}C^{\alpha}$ and ^{13}CO spins is converted to antiphase coherence on the ^{13}CO spin by a pair of 90° ^{15}N and ^{13}CO pulses prior to the ^{13}CO labeling period (t_1). At time c, the density operator is given by:

$$\begin{aligned}\sigma_c = &-4N_{(i)z}C^{\alpha}_{(i)z}C'_{(i-1)y}\Gamma_{(i)}(\delta)\cos(\Omega_{C'(i-1)}t_1)\\ &-4N_{(i)z}C^{\alpha}_{(i-1)z}C'_{(i-1)y}\Gamma_{(i-1)}(\delta)\cos(\Omega_{C'(i-1)}t_1)\end{aligned} \tag{4}$$

in which the ^{13}CO chemical shift is given by $\Omega_{C'(i-1)}$. The non-resonant phase shift of the ^{13}CO coherence due to the $^{13}C^{\alpha}$ 180° pulse during t_1 is compensated by adjusting the phase of the ^{13}CO 90° pulse at point c (McCoy and Mueller, 1992). The ^{13}CO antiphase coherence is converted to three-spin longitudinal order by application of a 90° carbonyl pulse. A gradient pulse is used to dephase unwanted coherences.

A 90° $^{13}C^{\alpha/\beta}$ pulse converts the longitudinal three-spin order into transverse $^{13}C^{\alpha}$ magnetization antiphase with respect to the ^{13}CO and ^{15}N. The density operator evolves under the $J_{C^{\alpha}C^{\beta}}$ scalar coupling Hamiltonian during the period 2η to effect transfer of the $^{13}C^{\alpha}$ magnetization to $^{13}C^{\beta}$. Efficient inversion of $^{13}C^{\alpha/\beta}$ spins without perturbing the ^{13}CO spins is achieved by application of a 180° band-selective pulse such as REBURP (Geen and Freeman, 1991) or rSNOB (Kupče et al., 1995). The relevant operators at point d are:

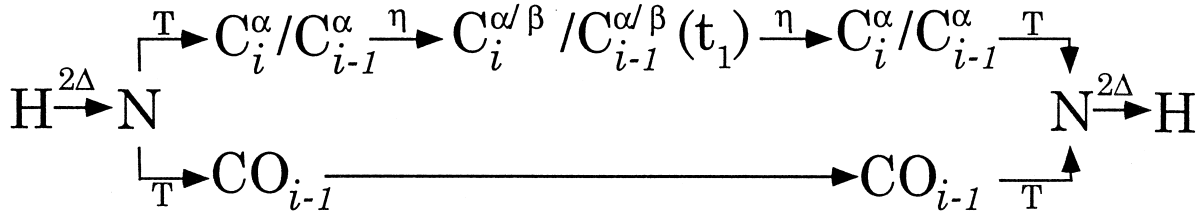

Figure 2. Coherence transfer pathway for the CO_H(N)CACB experiments shown in Figure 1. The simultaneous transfer to and from the CO and C^{α} spins during the periods T is depicted by parallel paths.

$$\begin{aligned}\sigma_d \;=\; & -4N_{(i)z}C^{\alpha}_{(i)y}C'_{(i-1)z}\Gamma_{(i)}(\delta)\\ & \times\cos(2\pi J_{C^{\alpha}C\beta}\eta)\cos(\Omega_{C'(i-1)}t_1)\\ & -4N_{(i)z}C^{\alpha}_{(i-1)y}C'_{(i-1)z}\Gamma_{(i-1)}(\delta)\\ & \times\cos(2\pi J_{C^{\alpha}C\beta}\eta)\cos(\Omega_{C'(i-1)}t_1)\\ & +8N_{(i)z}C^{\alpha}_{(i)x}C^{\beta}_{(i)z}C'_{(i-1)z}\Gamma_{(i)}(\delta)\\ & \times\sin(2\pi J_{C^{\alpha}C\beta}\eta)\cos(\Omega_{C'(i-1)}t_1)\\ & +8N_{(i)z}C^{\alpha}_{(i-1)x}C^{\beta}_{(i-1)z}C'_{(i-1)z}\Gamma_{(i-1)}(\delta)\\ & \sin(2\pi J_{C^{\alpha}C\beta}\eta)\cos(\Omega_{C'(i-1)}t_1)\end{aligned}\tag{5}$$

A 90° $^{13}C^{\alpha/\beta}$ pulse converts the density operator into a combination of transverse $^{13}C^{\alpha}$ and transverse $^{13}C^{\beta}$ coherences that evolve during the t_2 period. The carbonyl 180° refocussing pulse during t_2 introduces a non-resonant phase shift that is compensated for by a second carbonyl pulse inserted immediately prior to point e. At point e, the magnetization is given by

$$\begin{aligned}\sigma_e \;=\; & -4N_{(i)z}C^{\alpha}_{(i)y}C'_{(i-1)z}\Gamma_{(i)}(\delta)\cos(2\pi J_{C^{\alpha}C\beta}\eta)\\ & \times\cos(\Omega_{C'(i-1)}t_1)\cos(\Omega_{C^{\alpha}(i)}t_2)\\ & -4N_{(i)z}C^{\alpha}_{(i-1)y}C'_{(i-1)z}\Gamma_{(i-1)}(\delta)\cos(2\pi J_{C^{\alpha}C\beta}\eta)\\ & \times\cos(\Omega_{C'(i-1)}t_1)\cos(\Omega_{C^{\alpha}(i-1)}t_2)\\ & +8N_{(i)z}C^{\alpha}_{(i)z}C^{\beta}_{(i)x}C'_{(i-1)z}\Gamma_{(i)}(\delta)\cos(2\pi J_{C^{\alpha}C\beta}\eta)\\ & \times\cos(\Omega_{C'(i-1)}t_1)\cos(\Omega_{C^{\beta}(i-1)}t_2)\\ & +8N_{(i)z}C^{\alpha}_{(i-1)z}C^{\beta}_{(i-1)x}C'_{(i-1)z}\Gamma_{(i-1)}(\delta)\\ & \times\sin(2\pi J_{C^{\alpha}C\beta}\eta)\\ & \times\cos(\Omega_{C'(i-1)}t_1)\cos(\Omega_{C^{\beta}(i-1)}t_2)\end{aligned}\tag{6}$$

in which $\Omega_{C^{\alpha}_{(i)}}$ and $\Omega_{C^{\beta}_{(i)}}$ represent the $^{13}C^{\alpha}$ and $^{13}C^{\beta}$ chemical shifts of the ith residue. The above operators are restored to observable $^1H^N$ magnetization by reversing the transfer pathway used for their creation.

The constant time version of the pulse sequence, shown in Figure 1b, diverges from the basic version of the pulse sequence at point c, where multiple quantum terms are generated by applying ^{15}N, $^{13}C^{\alpha/\beta}$, and ^{13}CO 90° pulses:

$$\begin{aligned}\sigma_c \;=\; & -4N_{(i)z}C^{\alpha}_{(i)y}C'_{(i-1)x}\Gamma_{(i)}(\delta)\cos(\Omega_{C'(i-1)}t_1)\\ & -4N_{(i)z}C^{\alpha}_{(i-1)x}C'_{(i-1)x}\Gamma_{(i-1)}(\delta)\cos(\Omega_{C'(i-1)}t_1)\end{aligned}\tag{7}$$

The ^{13}CO chemical shift labeling occurs between points c and f of Figure 1b, concomitantly with the $^{13}C^{\alpha/\beta}$ transfer and t_2 evolution periods. As described in the caption to Figure 1, the ^{13}CO chemical shift evolution is refocussed during t_2 using a shaped Gaussian 180° pulse with a profile modulated to compensate for the non-resonant phase shift on the $^{13}C^{\alpha}$ and $^{13}C^{\beta}$ resonances (McCoy and Mueller, 1992).

The net duration of the chemical shift evolution period for the ^{13}CO magnetization between points c and f is given by

$$\begin{aligned}&(\eta-t_1/4)-t_1/4-t_1/4+(\eta-t_1/4)+\zeta+t_2/2\\ &-t_2/2-\eta-\eta=-t_1+\zeta\end{aligned}\tag{8}$$

The $J_{NC'}$ scalar coupling is refocussed between points c and f, the $J_{C^{\alpha}C'}$ scalar coupling is refocussed separately in each of the periods from points c to d, d to e, and e to f. The $J_{NC^{\alpha}}$ scalar coupling interaction is not refocussed during t_2 because two additional 180° ^{15}N pulses would be required. For a maximum value of $t_2 < 8$ ms, evolution of the density operator due to this unresolved scalar coupling results in a negligible increase in the F2 linewidths.

The CO_H(N)CACB sequence has been demonstrated on a 1.2 mM sample of $^{13}C/^{15}N$-labeled ubiquitin (VLI Research) in 50 mM potassium phosphate buffer (90% H_2O/10% D_2O) at pH = 5.8 and T = 300 K. The experiment was performed on a Bruker DRX-600 spectrometer equipped with a triple resonance three-axis gradient probe. Separate rf synthesizers were used for generation of the ^1H, ^{15}N, $^{13}C^{\alpha/\beta}$

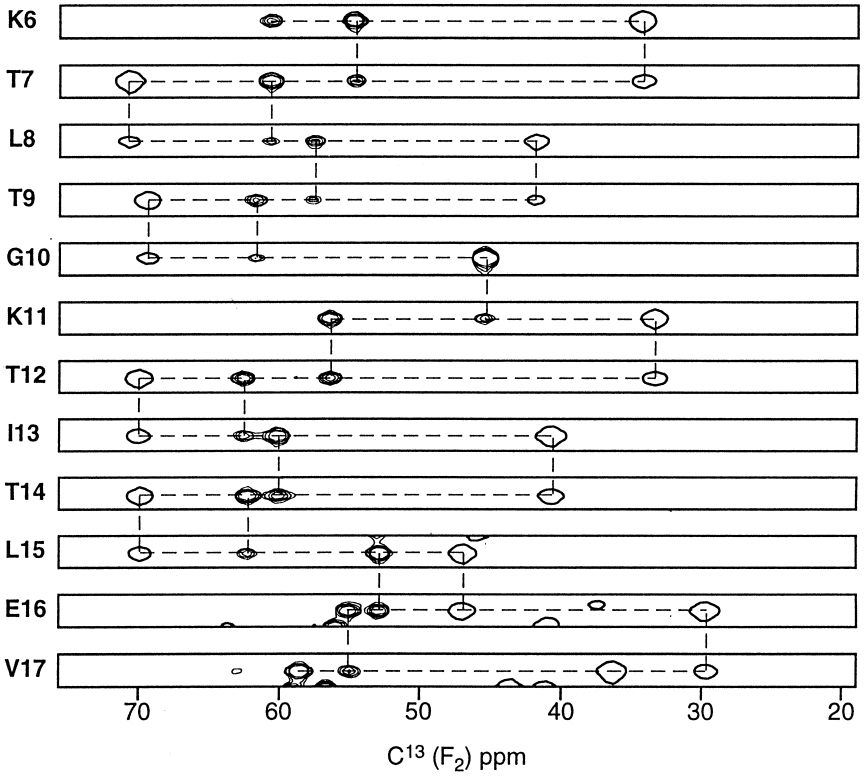

Figure 3. Twelve strip plots taken from the 3D CO_H(N)CACB spectrum of ubiquitin acquired with the pulse sequence of Figure 1a. F3($^1H^N$)/F2($^{13}C^{\alpha/\beta}$) slices taken at the F1(^{13}CO) frequencies for residues 6 through 17 are shown. The correlations to $^{13}C^{\alpha}$ resonances have positive intensities and are displayed with multiple contour levels, while the $^{13}C^{\beta}$ resonances have negative intensities and are displayed as a thicker single contour line. The CO_H(N)CACB spectrum consisted of 32 (t_1) × 64 (t_2) × 2048 (t_3) complex points with spectral widths of 1666 Hz (^{13}CO) × 9225 Hz ($^{13}C^{\alpha/\beta}$) × 10000 Hz (^1H)), giving total evolution times for t_1 and t_2 of 19.2 ms and 6.84 ms, respectively. The experiment was acquired for 50 h using 16 scans per complex point. Residual solvent signal was suppressed in the acquisition dimension using a convolution difference filter (Marion et al., 1989a) followed by polynomial baseline correction. The data were apodized using a Kaiser filter function in the ^{13}CO t_1 and $^{13}C^{\alpha/\beta}$ t_2 dimensions and exponential line broadening in the directly acquired ^1H t_3 dimension. The ^{13}CO t_1 and $^{13}C^{\alpha/\beta}$ t_2 interferograms were doubled in length by HSVD linear prediction (Barkhuijsen et al., 1987), using in-house software.

and ^{13}CO pulses. The carrier frequencies were centered at $^1H = 4.73$ ppm, $^{15}N = 119.4$ ppm, $^{13}C^{\alpha} = 60.3$ ppm, $^{13}C^{\alpha/\beta} = 45.4$ ppm and $^{13}CO = 177.9$ ppm. The $^{13}C^{\alpha/\beta}$ and ^{13}CO synthesizer outputs were combined and amplified using a 300 W linear amplifier (American Microwave Technologies). All data was processed using Felix 2.3 (Molecular Simulations).

Representative strip plots with axes corresponding to the F2($^{13}C^{\alpha/\beta}$)/F3(^1H) dimensions are shown in Figure 3. The resonance assignments for ubiquitin have been previously published (Grzesiek and Bax, 1993a; Wang et al., 1995). Each strip displays both the interresidue $^{13}C^{\alpha}_{(i)}$ and $^{13}C^{\beta}_{(i)}$ cross peaks and the intraresidue $^{13}C^{\alpha}_{(i-1)}$ and $^{13}C^{\beta}_{(i-1)}$ cross peaks. The $^{13}C^{\beta}$ cross peaks have opposite signs relative to the $^{13}C^{\alpha}$ cross peaks, as shown in Equation (6). The inter- and intraresidue cross peaks are distinguished by the differences in the $^1J_{NC^{\alpha}}$ and $^2J_{NC^{\alpha}}$ scalar couplings, which generally result in the intraresidue peak intensities being greater than the interresidue peak intensities.

Although the experiment shown in Figure 1a is conceptually straightforward, the constant time version of the pulse sequence, shown in Figure 1b, is preferable in practice. The two pulse sequences have the same number of 90° and 180° pulses; consequently, no additional losses of magnetization are expected in the constant time version due to rf inhomogeneity or off-resonance effects. Experimental spectra confirm that the signal-to-noise ratio in the first ^{13}CO plane ($t_1 = 0$) is identical for the two pulse sequences (data not shown). Although the maximum evolution period in the constant time experiment is limited to 4η ($\sim$ 16 ms), the signal does not decay as the ^{13}CO

labeling period is incremented and the data set can be resolution enhanced by mirror image linear prediction (Zhu and Bax, 1990).

The sensitivity of the constant time CO_H(N)CACB experiment (Figure 1b) compared to a sensitivity enhanced version of the HNCACB experiment is given by

$$\Lambda = \sin^2(2\pi {}^1J_{NC'}\delta)\exp(-2R_{2C'}\eta)\varepsilon \qquad (9)$$

in which $R_{2C'}$ is the transverse relaxation rate of the ^{13}CO spin and $1 \leq \varepsilon \leq 1.4$ is the efficiency of the sensitivity enhancement element (Palmer et al., 1991). For a protein with a rotational correlation time of 8 ns, corresponding to a molecular mass of approximately 15 to 20 kDa, Λ ranges from 0.6 to 0.85. In larger proteins, deuterium labeling may be required to reduce transverse relaxation rates of the $^{13}C^{\alpha}$ and $^{13}C^{\beta}$ resonances (LeMaster, 1990); in such cases, a ^2H decoupling sequence should be added between points c and f in Figure 1 (Grzesiek et al., 1993). The CO_H(N)CACB experiment also can be executed in a four-dimensional manner by frequency labeling both ^{15}N and ^{13}CO resonances. In this case, the ^{15}N is frequency labeled during the 2δ period following point f. By using the sensitivity enhancement technique for ^{15}N coherence selection (Palmer et al., 1991; Kay et al., 1992), the $\sqrt{2}$ signal loss normally associated with extension from three to four dimensions is avoided.

A CBCA(CO)NH (Grzesiek and Bax, 1992) experiment often is employed in conjunction with the HNCACB experiment to distinguish inter- from intraresidue cross peaks. An analogous companion for the CO_H(N)CACB can be obtained by straightforward modification of the CBCA(CO)NH pulse sequence to frequency label the ^{13}CO spins instead of the amide ^{15}N spins.

In summary, we have presented the CO_H(N)CACB experiment for establishing sequential resonance assignments by correlating the $^1H^N$ and ^{13}CO spins with the $^{13}C^{\alpha}$ and $^{13}C^{\beta}$ spins of adjacent amino acids. The experiment should prove useful when degeneracy in the ^{15}N resonances hinders the application of ^{15}N-based assignment strategies.

Acknowledgements

We thank Lynn McNaughton for technical support. This work was supported by the National Institutes of Health, Grant GM-50291 awarded to A.G.P., and a National Institutes of Health Postdoctoral Fellowship (GM17562) awarded to C.B. N.S.A. was supported by National Institutes of Health (National Institute of General Medical Science) Grant T32GM08281.

References

Barkhuijsen, H., de Beer, R. and van Ormondt, D. (1987) *J. Magn. Reson.*, **73**, 553–557.
Clubb, R.T., Thanabal, V. and Wagner, G. (1992) *J. Magn. Reson.*, **97**, 213–217.
Engelke, J. and Rüterjans, H. (1997) *J. Biomol. NMR*, **9**, 63–78.
Geen, H. and Freeman, R. (1991) *J. Magn. Reson.*, **93**, 93–141.
Grzesiek, S., Anglister, J., Ren, H. and Bax, A. (1993) *J. Am. Chem. Soc.*, **115**, 4369–4370.
Grzesiek, S. and Bax, A. (1992) *J. Am. Chem. Soc.*, **114**, 6291–6293.
Grzesiek, S. and Bax, A. (1993a) *J. Magn. Reson.*, **B102**, 103–106.
Grzesiek, S. and Bax, A. (1993b) *J. Biomol. NMR*, **3**, 185–204.
Kay, L.E., Ikura, M., Tschudin, R. and Bax, A. (1990) *J. Magn. Reson.*, **89**, 496–514.
Kay, L.E., Keifer, P. and Saarinen, T. (1992) *J. Am. Chem. Soc.*, **114**, 10663–10665.
Kupče, E., Boyd, J. and Campbell, I.D. (1995) *J. Magn. Reson.*, **B106**, 300–303.
LeMaster, D.M. (1990) *Q. Rev. Biophys.*, **23**, 113–174.
Löhr, F., Blumel, M., Schmidt, J.M. and Rüterjans, H. (1997) *J. Biomol. NMR*, **10**, 107–118.
Marion, D., Ikura, M. and Bax, A. (1989a) *J. Magn. Reson.*, **84**, 425–430.
Marion, D., Ikura, M., Tschudin, R. and Bax, A. (1989b) *J. Magn. Reson.*, **85**, 393–399.
McCoy, M.A. and Mueller, L. (1992) *J. Magn. Reson.*, **99**, 18–36.
Messerle, B.A., Wider, G., Otting, G., Weber, C. and Wüthrich, K. (1989) *J. Magn. Reson.*, **85**, 608–613.
Morris, G.A. and Freeman, R. (1979) *J. Am. Chem. Soc.*, **101**, 760–762.
Packer, K.J. and Wright, K.M. (1983) *Mol. Phys.*, **50**, 797–813.
Palmer, A.G. (1997) *Curr. Opin. Struct. Biol.*, **7**, 732–737.
Palmer, A.G., Cavanagh, J., Wright, P.E. and Rance, M. (1991) *J. Magn. Reson.*, **93**, 151–170.
Shaka, A.J., Barker, P.B. and Freeman, R. (1985) *J. Magn. Reson.*, **64**, 547–552.
Shaka, A.J., Keeler, J., Frenkiel, T. and Freeman, R. (1983) *J. Magn. Reson.*, **52**, 334–338.
Sørensen, O.W., Eich, G.W., Levitt, M.H., Bodenhausen, G. and Ernst, R.R. (1983) *Prog. NMR Spectrosc.*, **16**, 163–192.
Szyperski, T., Braun, D., Fernandez, C., Bartels, C. and Wüthrich, K. (1995) *J. Magn. Reson.*, **B108**, 197–203.
van de Ven, F.J.M. and Hilbers, C.W. (1983) *J. Magn. Reson.*, **54**, 512–520.
Wang, A.C., Grzesiek, S., Tschudin, R., Lodi, P.J. and Bax, A. (1995) *J. Biomol. NMR*, **5**, 376–382.
Wishart, D.S., Sykes, B.D. and Richards, F.M. (1991) *J. Mol. Biol.*, **222**, 311–333.
Wittekind, M. and Mueller, L. (1993) *J. Magn. Reson.*, **B101**, 201–205.
Zhu, G. and Bax, A. (1990) *J. Magn. Reson.*, **90**, 405–410.